Environmental Science and Pollution Research (2023) 30:96114–96124
https://doi.org/10.1007/s11356-023-29115-2

RESEARCH ARTICLE

Amine-functionalized reduced graphene oxide-supported silver nanoparticles for superior catalytic reduction of organic pollutants

Vijina C[1] · Majitha KP[1] · Shima P. Damodaran[1]

Received: 23 June 2023 / Accepted: 29 July 2023 / Published online: 11 August 2023

Abstract

In this work, a simple and environmentally friendly approach has been followed to synthesize amine-functionalized reduced graphene oxide (RGO)-supported silver nanoparticle (AgNPs) having superior catalytic efficiency towards the reduction of organic pollutants. RGO/AgNPs nanohybrid was synthesized by a one-pot hydrothermal reduction of silver nitrate in the presence of amino-propyl trimethoxy silane (APTMS)-functionalized graphene oxide (GO) nanosheets. The structural and morphological characterization of as-synthesized RGO/AgNPs nanohybrid was done by using XRD, SEM, TEM, FT-IR, and Raman spectroscopy techniques. APTMS plays an important role in controlling the size of anchored AgNPs on the nanohybrid in the present study. The $-NH_2$ groups on the surface of APTMS-modified GO function as effective and well-organized nucleation centers facilitating uniform growth of discrete and smaller-sized spherical AgNPs on the surface of RGO nanosheets. In the absence of APTMS, the nanohybrid comprised of bigger-sized AgNPs with few hundred of nanometers in dimension. The catalytic efficiency of RGO/AgNPs nanohybrid was evaluated for the reduction of two model organic pollutants: 4-nitrophenol (4-NP) and methylene blue (MB). Due to the synergistic effects of RGO, APTMS, and Ag components, RGO/AgNPs nanohybrid developed in the present study exhibited superior catalytic activity towards the reduction of 4-NP and MB in comparison with previously reported graphene/graphene oxide/reduced graphene oxide-supported AgNPs catalysts. The catalytic reduction of 4-NP and MB followed pseudo-unimolecular kinetics and the rate constants were found to be 18.83×10^{-3} s^{-1} and 131.5×10^{-3} s^{-1} respectively for 4-NP and MB. Furthermore, RGO/AgNPs nanohybrid showed admirable recyclability with negligible loss in its activity until five recycle runs. The superior catalytic activity, favorable kinetic parameters, and sustained catalytic efficiency after recycling make RGO/AgNPs nanohybrid a promising catalyst for the reduction of organic pollutants in environmental remediation.

Keywords Reduced graphene oxide · Silver nanoparticles · Nanohybrid · Catalytic reduction · 4-Nitrophenol · Methylene blue

Introduction

The discharge of huge volumes of wastewater containing harmful chemical effluents such as organic dyes, heavy metal ions, and other toxic chemicals is a major threat to the environment, and human beings (Adel et al. 2022). The presence of dyes and phenolic molecules contaminates the water reservoirs and adversely affects the health of humans and other aquatic organisms. 4-Nitrophenol (4-NP) and methylene blue (MB) are two such chemicals that have fatal effects on the health of organisms and the balance of ecosystems. 4-Nitrophenol is widely used in pesticides, fungicides, dyes, explosives, and pharmaceutical industries (Nezamzadeh-Ejhieh and Khorsandi 2014). Despite its wide range of applications, 4-NP is a harmful chemical and can cause extensive damage to the environment and living systems on account of its toxicity and high stability. Acute exposure to 4-NP can cause multiple health issues in humans including nausea, drowsiness, cyanosis, and headache (Sponza and Kuscu 2011). MB is an aromatic heterocyclic dye that is mainly used in the textile, paper, printing, food, and pharmaceutical industries (Low and Tan 2018). It is a hazardous chemical and can cause carcinogenic, teratogenic, and mutagenic

Responsible Editor: George Z. Kyzas

✉ Shima P. Damodaran
shimachem@kannuruniv.ac.in; shimapd@gmail.com

[1] Department of Chemistry, Kannur University, Kannur, Kerala 670 327, India

health problems in humans (Khan et al. 2022). On account of their persistent nature and non-biodegradability, both 4-NP and MB are harmful to the aquatic biota and can disrupt the aquatic ecosystem. The effective removal/reduction of 4-NP and MB from the wastewater or their transformation into non-hazardous molecules is of great practical importance in this regard.

Various methods were tried for the removal of these chemicals from wastewater including adsorption, photocatalysis, electrochemical reduction, oxidation, precipitation, membrane filtration, and catalytic reduction (Katheresan et al. 2018). Among the above-mentioned techniques, the catalytic reduction is a promising and widely used method on account of its simplicity, cost-effectiveness, environmental friendliness, mild, safe, and sludge-free operations (Mohammadi and Entezari 2018). The catalytic reduction will convert the harmful organic pollutants of wastewater to less-toxic chemicals and thereby helps in attaining an eco-friendly aquatic environment. On account of their unique size-dependent physical, chemical, and catalytic properties, different nanomaterials have been widely used for the catalytic reduction of organic pollutants. Noble metal nanoparticles have emerged as promising materials for catalysis in this regard, because of their high surface area, biocompatibility, oxidation resistance., and high electrical conductivity (Hervés et al. 2012). Among different noble metal nanoparticles, silver nanoparticles (AgNPs) provide efficient electron transfer reactions and received more scientific attention for catalytic reduction in recent years (Shaker Ardakani et al. 2021). However, bare silver nanoparticles are prone to aggregation due to their large surface energy. The aggregation process can significantly reduce the catalytic activity of silver nanoparticles (Jiang et al. 2005). Furthermore, on account of their smaller size, it will be difficult to separate and recover these nanoparticles from the reaction medium after the reduction process. To overcome the above-mentioned disadvantages, silver nanoparticles can be immobilized on suitable supporting materials. An ideal supporting material should have a high surface area for the effective dispersion of nanoparticles to prevent their aggregation and it should also possess high electrical conductance to improve the catalytic activity of anchored metal nanoparticles while taking part in electron transport during the reduction process. Different materials like zeolites, polymers, hydrogels, carbon-based nanomaterials, metal-organic frameworks, and MXenes have been tried as supporting materials to prevent the aggregation of silver nanoparticles (Ndolomingo et al. 2020). Among them, carbon-based nanomaterials such as graphene (G), graphene oxide (GO), reduced graphene oxide (RGO), and carbon nanotubes (CNTs) have been demonstrated as promising supporting materials for AgNPs due to their large surface area, high electron mobility, and excellent mechanical stability (Karczmarska et al. 2022). Owing to their good water dispersibility and the presence of a large number of oxygen-containing functional groups, GO and RGO outperform both G and CNTs in wastewater treatment (Yu 2020). Additionally, GO and RGO can be synthesized on a large scale from low-cost reactants (Trikkaliotis et al. 2021). As the electrical conductivity of RGO is higher than that of GO, it can function as a better catalytic component for the reduction of organic pollutants. Furthermore, RGO can efficiently adsorb the organic molecules on its surface by π-π interactions and electrostatic interactions arising from its abundant oxygen-containing functional groups. The adsorption will bring the organic pollutants to the proximity of anchored metal catalytic centers which can accelerate the reduction process. The above-mentioned features make RGO an ideal supporting material for AgNPs towards the catalytic reduction of organic pollutants in comparison with other carbon-based nanomaterials.

An ideal RGO-Ag nanohybrid catalyst should have a homogenous distribution of discrete AgNPs on the surface of RGO. By enhancing the surface electron density of anchored AgNPs, superior catalytic efficiency can be attained for such RGO-Ag nanohybrids. In the present study, APTMS was employed for the dual role of controlling the size of anchored AgNPs and increasing their surface electron density. We developed a facile and environmentally friendly approach for the fabrication of aminopropyl trimethoxy silane (APTMS)-functionalized RGO-supported silver nanoparticles having a uniform distribution of discrete and smaller-sized AgNPs as an efficient catalytic platform for the reduction of organic pollutants. GO was synthesized by a modified Hummers method and it was subsequently surface functionalized with APTMS. RGO/AgNPs nanohybrid was synthesized by a one-pot hydrothermal citrate reduction of silver salt solution in the presence of APTMS-modified GO nanosheets. The structure and morphology of RGO/AgNPs nanohybrid were characterized in detail using scanning electron microscopy (SEM), transmission electron microscopy (TEM), X-ray diffraction (XRD), Fourier-transform infrared spectroscopy (FT-IR), and Raman spectroscopy. The catalytic efficiency of RGO/AgNPs nanohybrid was evaluated for the reduction of 4-NP and MB using sodium borohydride ($NaBH_4$) as the reducing agent in aqueous media at room temperature. The reduction processes were monitored over time using UV-Vis spectroscopy. The kinetics of reduction reactions and the reusability of the nanohybrid was also studied. Due to the unified effects of RGO, APTMS, and Ag components, RGO/AgNPs nanohybrid exhibited excellent catalytic activity towards the 4-NP and MB at ambient conditions. The calculated rate constants for the reduction of 4-NP and MB in the present study were significantly higher in comparison with the rate constants reported for other G/GO/RGO-supported metal nanoparticles.

Experimental details

Materials

Graphite powder, sulphuric acid (H_2SO_4), sodium nitrate ($NaNO_3$), potassium permanganate ($KMnO_4$), hydrogen peroxide (H_2O_2), hydrochloric acid (HCl), ethanol, APTMS, silver nitrate ($AgNO_3$), trisodium citrate dihydrate, ethylene glycol, $NaBH_4$, 4-nitrophenol, and methylene blue were purchased from Merck India. All the chemicals were used as received without any further purification. Deionized water was used for all experiments in the present study.

Synthesis of graphene oxide

GO was synthesized by a modified Hummer's method (Hummers and Offeman 1958). For the synthesis, 2 g of graphite powder was dispersed in 92 ml of concentrated H_2SO_4 by magnetic stirring. Then, 2 g of $NaNO_3$ was added into the dispersion followed by 12 g of $KMnO_4$. The temperature of the reaction mixture was maintained below 10 °C and the stirring was continued for 12 h. The reaction mixture was then diluted by adding 370 ml of distilled water by keeping the reaction vessel in an ice bath. Subsequently, 20 ml of H_2O_2 was added to the mixture and stirring was continued for another 1 h. The product was finally washed with 10% HCl solution and deionized water to remove the impurities. The obtained GO was then dried in a vacuum oven for 7 h at 70 °C.

Synthesis of RGO/AgNPs nanohybrid

One hundred milligrams of GO was dispersed in 50 ml of ethanol with the help of ultrasonication initially. To the above GO dispersion, about 1 ml of APTMS was added and the reaction mixture was magnetically stirred for 5 h. After the evaporation of ethanol, 30 ml of distilled water was added to the reaction mixture and was mixed well. The APTMS-modified GO dispersion was then mixed with 10 ml of 0.1 M $AgNO_3$ solution and 10 ml of 0.5 M trisodium citrate dihydrate solution. The reaction mixture was then transferred into a Teflon-lined stainless steel autoclave and heated at 120 °C for 6 h. The black precipitate obtained was washed with ethanol and deionized water several times and finally dried at 70 °C for 7 h in a vacuum oven. To check the role of APTMS, a control synthesis was also carried out under the same experimental conditions in the absence of APTMS.

Characterization techniques

XRD analysis was performed using Rigaku smart lab instrument using Cu Kα radiation (λ= 1.5418 Å). JEOL Model JSM − 6390LV electron microscope was used to record the SEM images. JEM-2010 (JEOL, Japan) transmission electron microscope at an accelerating voltage of 200 kV was used to perform the TEM analysis and selected area electron diffraction (SAED). FT-IR analysis was done using Thermo Scientific Nicolet iS5 spectrometer. Raman analysis was done using a Horiba Xplora micro-Raman spectrometer at 532 nm. The reduction of 4-NP and MB was monitored using analytical ultraviolet (UV)–visible (vis) spectrophotometer by recording the spectrum in the wavelength range of 200–800 nm.

Catalytic reduction of 4-nitrophenol and methylene blue

The catalytic performance of as-synthesized nanohybrid for the reduction of 4-NP and MB was studied using $NaBH_4$ as the reducing agent at room temperature. For the reduction studies, about 0.12 mM 4-NP solution was taken in a beaker, and to the above solution, 0.5 ml of 0.5 M $NaBH_4$ solution was added. The absorption of the reaction mixture without the catalyst was recorded using the UV-Vis spectrometer in the scanning range of 200 to 800 nm. About 0.2 mg/mL of RGO/AgNPs nanohybrid was added to the above reaction mixture and the reduction reaction was monitored by recording the decrease in intensity of the characteristic peak of 4-nitrophenolate anion at 400 nm. For the reduction studies of MB, a dye concentration of 0.025 mM and a catalyst concentration of 0.1 mg/mL were used. The reduction reaction of MB was monitored by recording the decrease in intensity of the characteristic peak of MB at 662 nm. To check the reusability, the RGO/AgNPs nanohybrid was recovered from the reaction medium after catalytic reduction with the help of centrifugation. It was then washed with ethanol and dried in a vacuum oven. The recycled RGO/AgNPs nanohybrid was used for the subsequent catalytic reduction cycles.

The percentage conversion of the analyte was calculated using Eq. (1)

$$\% \text{ conversion} = \frac{C_0 - C_e}{C_0} \times 100\% \quad (1)$$

where C_0 is the initial concentration and C_e is the final concentration of the analyte.

Results and discussion

Morphological and structural characterization of GO and RGO/AgNPs nanohybrid

The XRD patterns of graphite, GO, and RGO/AgNPs nanohybrid are presented in Fig. 1. Graphite has a sharp diffraction peak at $2\theta = 26.5°$ corresponding to (002) planes having

a d-spacing of 0.34 nm (Fig. 1a). The characteristic peak of graphite has disappeared after oxidation and the well-defined peak of GO has appeared at $2\theta = 10.7°$ (Fig. 1b) for the (001) reflections. The peak at $2\theta = 42.6°$ corresponds to the (111) plane of GO (Trikkaliotis et al. 2020). The d-spacing for GO was 0.83 nm, which is much higher than that of graphite, due to the presence of many oxygen-bearing functional groups on GO lattice. During the hydrothermal treatment, along with the formation of AgNPs, GO will be getting reduced to RGO. The XRD spectrum of RGO obtained by the hydrothermal reduction of GO (control experiment in the absence of silver nitrate) is shown in Fig. S1 where the characteristic (002) diffraction peak of RGO was observed at $2\theta = 25.5°$. The XRD pattern of the RGO/AgNPs nanohybrid (Fig. 1c) contains prominent peaks around $2\theta = 38°$, 44°, 65°, and 77° corresponding to (111), (200), (220), and (311) planes of crystalline FCC lattice of Ag respectively. The XRD pattern of RGO/AgNPs does not show the diffraction peaks corresponding to RGO, suggesting that the nanohybrid consists of disorderly stacked RGO nanosheets and well-crystalline Ag nanoparticles. Also, the quantity of such disorderly stacked RGO in the nanohybrid will be very small to perform its crystallinity in the XRD spectra.

Figure 2a and b depict the SEM and TEM images of GO, respectively. The results show that the GO synthesized through modified Hummer's method has a transparent wrinkled sheet-like structure. Figure 2c shows the TEM images of the as-synthesized RGO/AgNPs nanohybrid. The nanohybrid consists of well-organized distribution of discrete and spherical silver nanoparticles on the surface of RGO nanosheets. Figure 3a shows the size distributions of AgNPs obtained from TEM image analysis. The average particle size of anchored AgNPs was found to be ~23 nm. The SAED pattern of the RGO/AgNPs nanohybrid is given in Fig. 2d. Four discrete bright rings were observed in the SAED patterns, indicating the formation of a highly crystalline FCC structure of Ag nanoparticles anchored on the surface of RGO nanosheets. Each ring is formed by the diffractions from the (111), (200), (220), and (311) planes of metal nanoparticles, which are consistent with the XRD data.

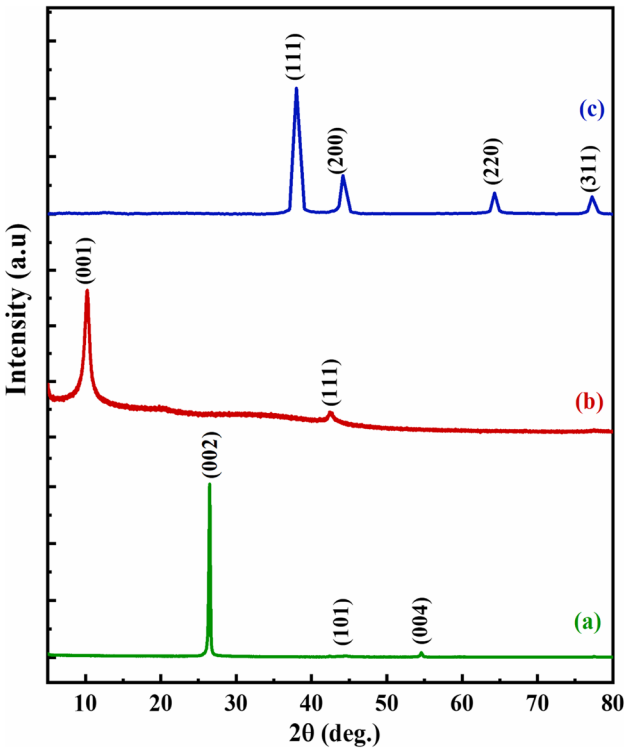

Fig. 1 The XRD patterns of **a** graphite, **b** GO, and **c** RGO/AgNPs nanohybrid

The APTMS plays an important role in controlling the size of anchored AgNPs on the nanohybrid. Figure 3b shows the TEM image of the RGO/AgNPs nanohybrid prepared in the absence of APTMS. As evident from the TEM image, the anchored nanoparticles are very big with few hundred of nanometers in dimension. The amine functional groups are known to have a high affinity for metal ions. In a recent report, graphene oxide modified with amine functional groups leads to stabilization and uniform distribution of palladium (Pd) NPs on the surface of GO (Saptal et al. 2019). In another report, APTMS-functionalized GO and RGO allowed rapid conversion of gold cations into AuNPs where residual groups of APTMS functioned as the active sites for the nucleation Au–GO nanocomposites (Pandey et al. 2016).

Figure 4 shows the schematic illustration of the synthesis of RGO/AgNPs nanohybrid in the present study. After surface functionalization with APTMS, the GO surface will have -NH_2 functional groups. These -NH_2 groups on the surface of APTMS-modified GO will act as effective and well-organized nucleation centers facilitating uniform growth of smaller-sized Ag nanoparticles. In the absence of APTMS, there will not be any such well-organized nucleation centers on the surface of GO which will result in the formation of bigger-sized Ag nanoparticles (Fig. 3b).

The APTMS binding on GO surface was confirmed by FT-IR analysis. Figure 5 shows the FT-IR spectra of bare and APTMS-modified GO. The FT-IR spectrum of GO (Fig. 5a) exhibits characteristic peaks at 3405, 1718, 1617, and 1232 cm^{-1} corresponding to O–H, C=O, C=C, and C–O–C stretching frequencies respectively (Damodaran 2021). The absorptions at 1380 and 1052 cm^{-1} correspond to the O=C–O and C–O stretching frequencies of the carboxy and alkoxy groups present on the surface of GO respectively. The FT-IR spectrum of APTMS-modified GO (Fig. 5b) exhibits two peaks at 2925 and 2865 cm^{-1} corresponding to the C-H symmetric and asymmetric stretching vibrations of propyl moieties of APTMS (Chen et al. 2015). The peaks at 1633 and 1587 cm^{-1} are attributed respectively to the N–H

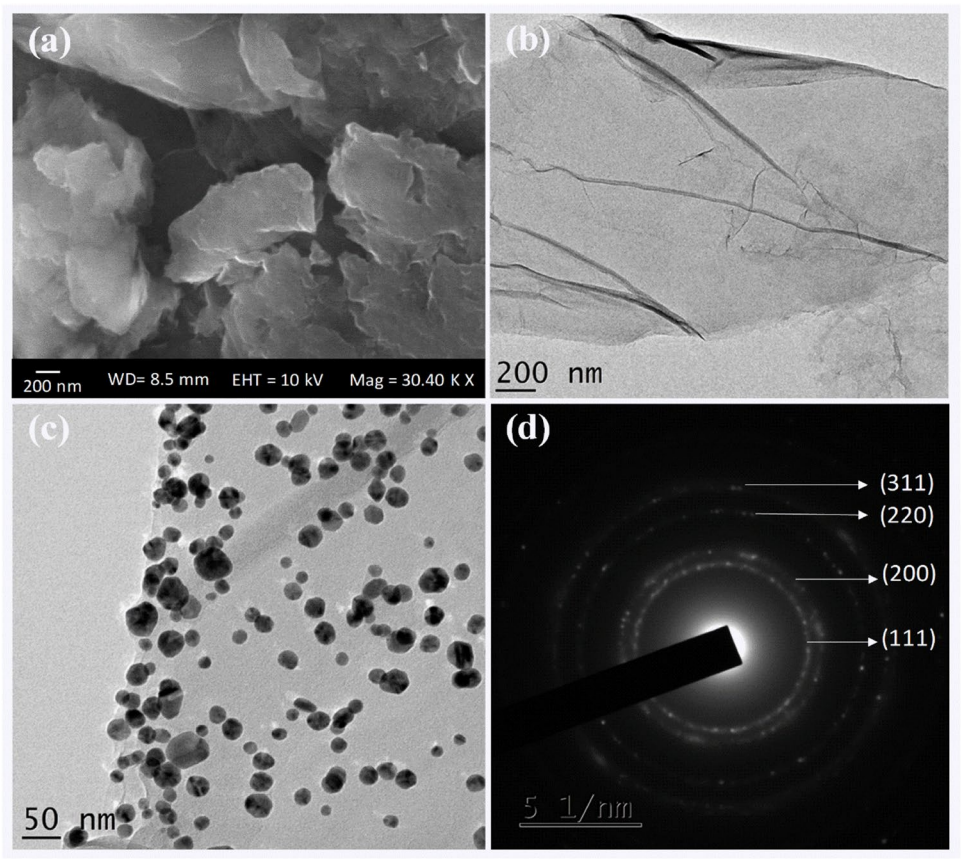

Fig. 2 The **a** SEM and **b** TEM images of GO, **c** TEM image, and **d** SAED pattern of RGO/AgNPs nanohybrid

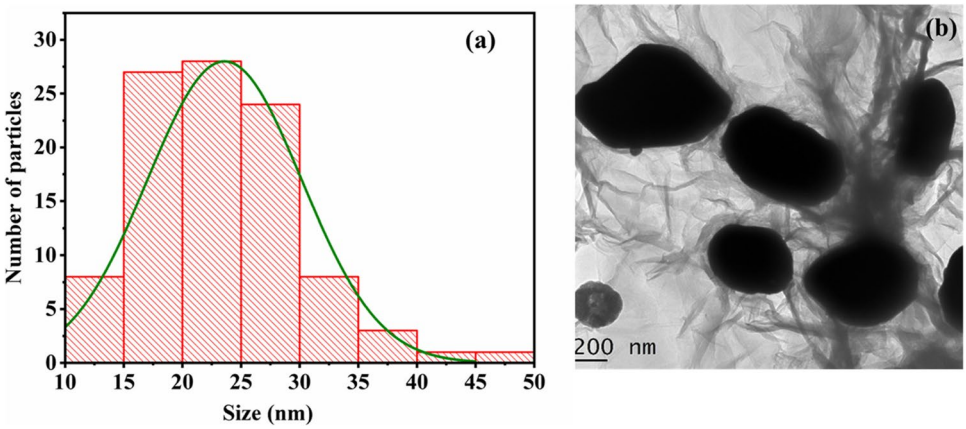

Fig. 3 **a** Size distribution of AgNPs in RGO/AgNPs nanohybrid synthesized using APTMS-modified GO. **b** TEM image of RGO/AgNPs nanohybrid synthesized in the absence of APTMS

deformation vibration of free amino groups and the N–H bending vibration of H-bonded amino groups of APTMS (Dong et al. 2019). The FT-IR spectrum of APTMS-modified GO also exhibits peaks corresponding to Si–O–C and Si–O–Si stretching vibrations at 1105 and 1052 cm^{-1} respectively (Chen et al. 2015). The presence of the above-mentioned characteristic peaks confirms the successful binding of APTMS on the surface of GO.

Figure 6 represents the Raman spectra of GO and RGO/AgNPs nanohybrid. The two prominent peaks appeared between 1200 and 1600 cm^{-1} corresponding to the characteristic D and G bands of graphene-based materials. The D band corresponds to the defects in the graphene-based sheets and the G band corresponds to the ordered vibrations of the sp^2 hybridized carbon structure of the sheets (Nimita Jebaranjitham et al. 2019). The ratio of intensity (I_D/I_G) gives an estimate of the defect intensity in graphene-based materials (Tran et al. 2020). The estimated peak intensity ratios I_D/I_G for GO and RGO/AgNPs were 0.849 and 0.983 respectively. As evident from the TEM image (Fig. 2c), the

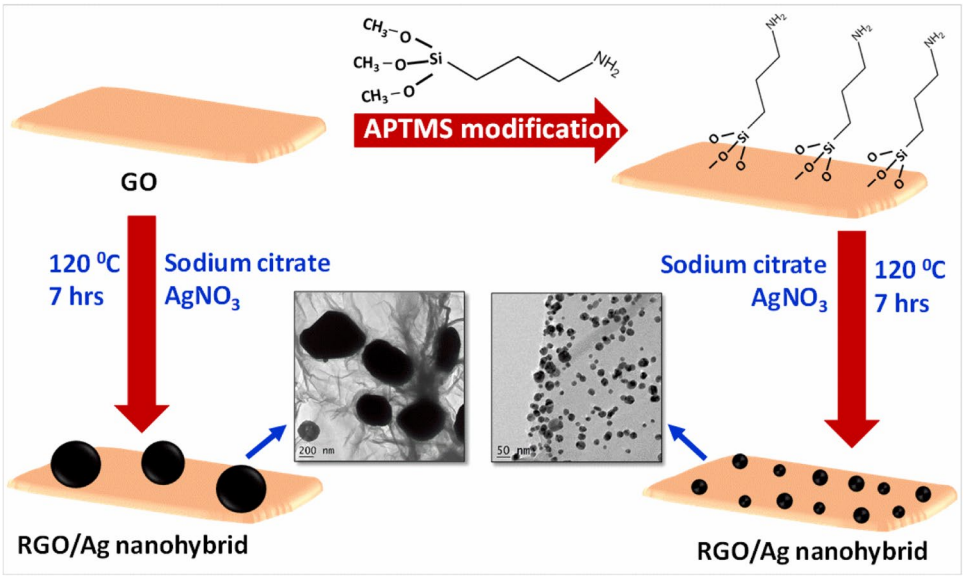

Fig. 4 Schematic illustration of the synthesis of RGO/AgNPs nanohybrid

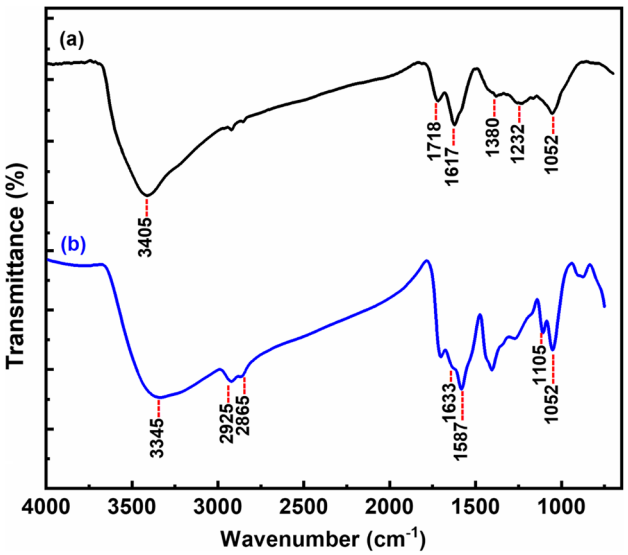

Fig. 5 The FT-IR spectra of **a** GO and **b** APTMS-functionalized GO

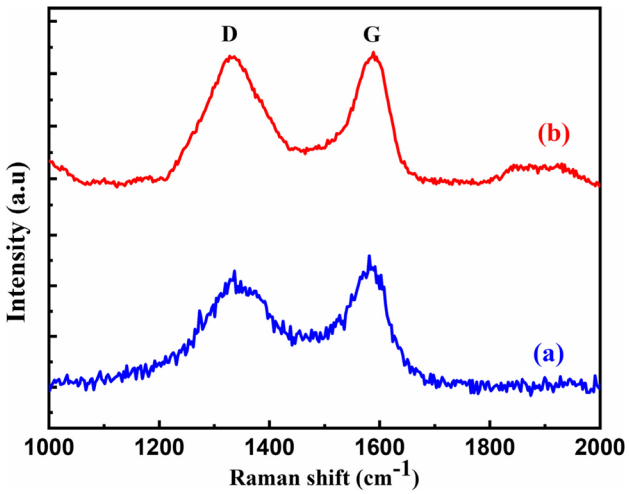

Fig. 6 The Raman spectra of **a** GO and **b** RGO/AgNPs nanohybrid

Ag nanoparticles are uniformly distributed on RGO to produce considerable defects in the RGO lattice, causing an increment in the I_D/I_G ratio.

Catalytic reduction of 4-nitrophenol

The catalytic activity of the as-synthesized RGO/AgNPs nanohybrid was examined for the reduction of 4-NP using $NaBH_4$ as the reducing agent at room temperature. The aqueous solution of 4-NP exhibits an absorption peak of around 317 nm, which had undergone a bathochromic shift after the addition of $NaBH_4$ (Fig. S2). The new peak appeared around 400 nm is due to the formation of 4-nitrophenolate anion. The color of the solution changed from light yellow to greenish yellow after the addition of $NaBH_4$. The intensity of the peak at 400 nm remained unchanged for a long time, indicating the reduction is very slow even with the strong reducing agent $NaBH_4$ (Fig. S3). When the RGO/AgNPs nanohybrid was added to the reaction mixture, the intensity of the peak of 4-nitrophenolate anion started decreasing instantly, and a new peak has appeared around 297 nm due to the formation of the reduction product 4-aminophenol. 0.2 mg/ml of RGO/AgNPs nanohybrid could reduce 0.12 mM of 4-NP solution almost completely within 95 s (Fig. 7a). The fast reaction kinetics shows that RGO/AgNPs nanohybrid can effectively promote the transport of electrons from sodium borohydride to 4-nitrophenol and thereby accelerate the reduction process. The concentration of $NaBH_4$ (0.5 M) was very high in comparison with 4-NP (0.12 mM) in the

present study. The relatively higher concentration of $NaBH_4$ will keep the concentration of BH_4^- unaltered during the reduction. Thus, the pseudo-first-order kinetic model can be used to evaluate the rate constant of catalytic reduction. The rate constant (k) of the reaction could be determined from the kinetic plot of ln (C_0/C) versus time (t) in seconds, using Eq. (2).

$$\ln\left(\frac{A}{A_0}\right) = \ln\left(\frac{C}{C_0}\right) = -kt \quad (2)$$

where C_0 and A_0 are the concentration and corresponding absorbance respectively of the analyte at time t = 0. C and A are the concentration and corresponding absorbance respectively of the analyte at time t.

An excellent linear correlation of ln (C_0/C) versus time (t) is shown in Fig. 7b. The kinetic rate constants were calculated from the slope of the linear fit. For RGO/AgNPs nanohybrid, the k value was equal to 18.83×10^{-3} s^{-1}. Table 1 shows the comparison of the catalytic activity of as-synthesized nanohybrid with that of previously reported 4-NP reduction using G/GO/RGO-supported metal nanoparticles. The RGO/AgNPs nanohybrid synthesized in the present study shows excellent catalytic activity in comparison with previous reports on G/GO/RGO-supported metal nanoparticles.

Catalytic reduction of methylene blue

The catalytic activity of the as-synthesized RGO/AgNPs nanohybrid was also examined for the reduction of MB. The aqueous solution of MB exhibits an absorption peak at 662 nm. The intensity of the above peak remained unchanged after the addition of $NaBH_4$ for a long time, which indicates that the rate of the reduction process is low (Fig. S4). The intensity of the characteristic peak of MB reduced immediately after the addition of RGO/AgNPs nanohybrid. The nanohybrid exhibited excellent catalytic activity as evident from Fig. 8a. It took only 22 s for 0.2 mg/mL of RGO/AgNPs nanohybrid to reduce 0.12 mM MB solution completely. As the concentration of $NaBH_4$ (0.5 M) used was much higher than that of MB, the reduction of MB followed pseudo-first-order kinetics (Fig. 8b). The rate constant was evaluated from the kinetic plot of ln (C_0/C) versus time (t) in seconds, using equation (2). The estimated k value for MB reduction was 131.5×10^{-3} s^{-1} which is much better than the k values reported for G/GO/RGO-supported metal nanoparticles (Table 2).

The excellent catalytic activity of developed RGO/AgNPs nanohybrid is attributed to the unified effects of RGO, APTMS, and Ag components. The aggregation of nanoparticles is reported to cause a reduction in the catalytic activity of bare metal nanoparticles. In the present RGO/AgNPs nanohybrid, RGO nanosheets function as a supporting material for the effective dispersion of AgNPs which can prevent their aggregation and thereby retain their catalytic activity. RGO will also accelerate the reduction process by facilitating efficient adsorption of 4-NP and MB on its surface by π-π and electrostatic interactions arising from its oxygen-containing functional groups. Studies have shown that the presence of amine groups on the surface of GO nanosheets increases the surface electron density of anchored metal NPs by electron donation from the -NH_2 groups which accelerated the catalytic activity of the resulting nanohybrid (Saptal et al. 2019). Thus, the amine functional groups of APTMS present in the developed RGO/AgNPs nanohybrid will also augment the catalytic activity of anchored silver nanoparticles. Overall, immobilization of silver nanoparticles on the surface of RGO nanosheets will produce a large number of active-catalytic spots enabling an effectual contact between AgNPs and adsorbed organic pollutants for the reduction process. This synergistic effect of RGO, APTMS, and Ag components will accelerate the electron transfer from the donor (BH_4^- ion) to the acceptor molecules (4-NP or MB). During reduction, 4-NP will get converted into 4-aminophenol (Bae et al. 2016) and MB will convert to leucomethylene blue (Patel et al. 2022).

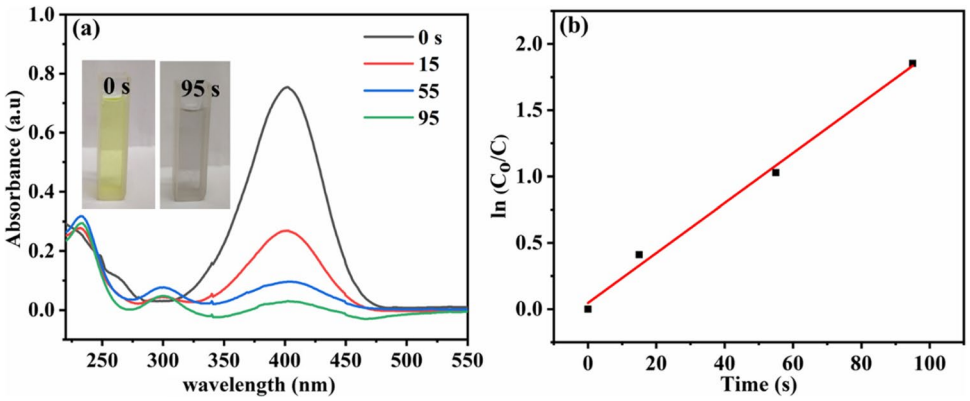

Fig. 7 **a** UV–vis spectra 4-NP with 0.5 M $NaBH_4$ in the presence of RGO/AgNPs. The corresponding plot of ln (C_0/C) against the reaction time for pseudo-first-order reduction kinetics is shown in **b**. Inset of **a** shows the solution of 4-NP + $NaBH_4$, before and after the addition of 0.2 mg/ml of RGO/AgNPs nanohybrid

Table 1 The comparison of the catalytic activity of RGO/AgNPs nanohybrid with previous reports on G/GO/RGO-supported metal nanoparticles towards the reduction of 4-NP.

Nanohybrid	k	Time (s)	Reference
GO/EDA/Ag NPs	3.345×10^{-4} s^{-1} mg^{-1}	1800	(Nimita Jebaranjitham et al. 2019)
GO/DAP/Ag NPs	7.548×10^{-4} s^{-1} mg^{-1}	720	(Nimita Jebaranjitham et al. 2019)
RGO/CNT/Fe/Ag	188.43×10^{-4} s^{-1} mg^{-1}	360	(Tran et al. 2020)
Ag/TPG	3.35×10^{-3} s^{-1}	720	(Wang et al. 2015)
Pd/G	2.35×10^{-3} s^{-1}	720	(Wang et al. 2014)
CG-Pt-1	0.974×10^{-3} s^{-1}	3600	(Chen and Chen 2018)
RGO/Ni	0.154×10^{-3} s^{-1}	4920	(Svalova et al. 2021)
CuO-RGO	2.5×10^{-3} s^{-1}	540	(K et al. 2019)
Ag/Au/RGO	3.47×10^{-3} s^{-1}	360	(Hareesh et al. 2016)
RGO/Fe_3O_4/Ag	6.17×10^{-3} s^{-1}	600	(Thu et al. 2017)
Au/G	3.17×10^{-3} s^{-1}	720	(Li et al. 2012)
RGO/Ag NP	6.295×10^{-3} s^{-1}	480	(Das et al. 2023)
RGO/QCP/Ag	19.283×10^{-3} s^{-1}	120	(Zhou et al. 2020)
Cu/Cu_2O/RGO	16.3×10^{-3} s^{-1}	360	(Xie et al. 2019)
AuNPs/RGO	1.96×10^{-3} s^{-1}	1080	(Li et al. 2019)
RGO/Ag_2O	-	120	(Iqbal et al. 2021)
AgNPs/RGO	-	540	(Kolya et al. 2019)
Ag-Ni/RGO	11.72×10^{-3} s^{-1}	240	(Han 2023)
Pd-Ni/RGO	2.667×10^{-3} s^{-1}	720	(Revathy et al. 2018)
Ag-Pd-PDA/RGO	5.4×10^{-3} s^{-1}	300	(Alipour and Namazi 2019)
Pt_1Co_3Ncs/N-RGO	12.35×10^{-3} s^{-1}	660	(Zhang et al. 2017)
RGO/AgNPs	18.83×10^{-3} s^{-1} (941.5×10^{-4} s^{-1} mg^{-1})	95	Present study

At the end of the catalytic process, the reduction products will leave the catalyst surface making the catalytic site available for the next cycle.

Reusability of the RGO/AgNPs nanohybrid

The reusability of heterogeneous catalysts is a crucial factor for their practical applications. The RGO/AgNPs catalyst developed in the present study was also investigated for its recyclability for 4-NP and MB reductions. To check the reusability, the RGO/AgNPs nanohybrid was recovered from the reaction medium after catalytic reduction and the recycled nanohybrid was used for the subsequent catalytic reduction cycles. The percentage of conversion of 4-NP and MB solutions using RGO/AgNPs nanohybrid for five consecutive cycles is presented in Fig. 9a and b, respectively. As shown in Fig. 9a, the conversion efficiency of RGO/AgNPs for the reduction of 4-NP was above 98% for the first three cycles and was above 84% even after the fifth cycle. Figure 9b shows that the percent conversion of MB using RGO/AgNPs was nearly 100% for the first cycle, and then decreased to 95% in the second cycle. The percent conversion was nearly the same for the remaining 3 cycles. The above results prove that RGO/AgNPs nanohybrid is an excellent recyclable catalyst for the reduction of 4-NP and MB.

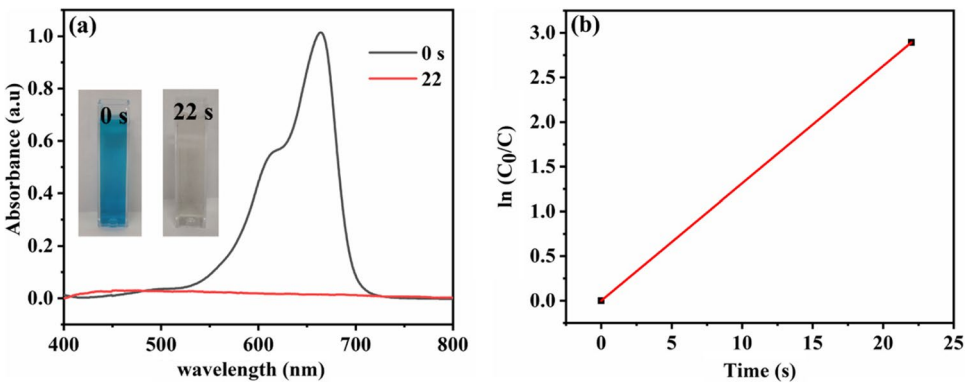

Fig. 8 **a** UV–vis spectra of MB with 0.5 M $NaBH_4$ in the presence of RGO/AgNPs nanohybrid. The corresponding plot of ln (C_0/C) against the reaction time for pseudo-first-order reduction kinetics is shown in **b**. Inset of **a** shows the solution of MB + $NaBH_4$, before and after the addition of 0.2 mg/ml of RGO/AgNPs nanohybrid

Table 2 The comparison of the catalytic activity of RGO/AgNPs nanohybrid with previous reports on G/GO/RGO-supported metal nanoparticles towards the reduction of MB

Nanohybrid	*k*	Time (s)	Reference
Ag/Fruit extract	-	600	(Saha et al. 2017)
Co/RGO	-	3000	(Krishna et al. 2016)
Graphene hydrogel/Cu	0.127 s^{-1}	30	(Zelechowska et al. 2016)
Magnetic GO/Ag	7.5×10^{-3} s^{-1}	600	(Doan et al. 2021)
Pd/RGO-A.abrotanum	0.049 s^{-1}	40	(Hashemi Salehi et al. 2019)
RGO/Ag NPs	-	480	(Sahu et al. 2019)
G/Ag	0.23×10^{-3} s^{-1}	1800	(He et al. 2016)
RGO/Fe_3O_4	-	720	(Vinothkannan et al. 2015)
GO/Ag	0.63×10^{-3} s^{-1}	900	(Sreekanth et al. 2016)
Ag/RGO	2.6×10^{-3} s^{-1}	2400	(Dat et al. 2020)
RGO/QCP/Ag	20.6×10^{-3} s^{-1}	125	(Zhou et al. 2020)
RGO/Ag	7.5×10^{-3} s^{-1}	225	(Zhou et al. 2020)
Ag/3D-RGO	13.93×10^{-3} s^{-1}	-	(Han et al. 2022)
Ag-Ni/RGO	4.14×10^{-3} s^{-1}	420	(Han 2023)
Ag/RGO	0.23×10^{-3} s^{-1}	1800	(He et al. 2016)
Ag NPs/F-RGO	24×10^{-3} s^{-1}	70	(Zarei et al. 2021)
RGO/AgNPs	131.5×10^{-3} s^{-1} (6575×10^{-4} s^{-1} mg^{-1})	22	Present study

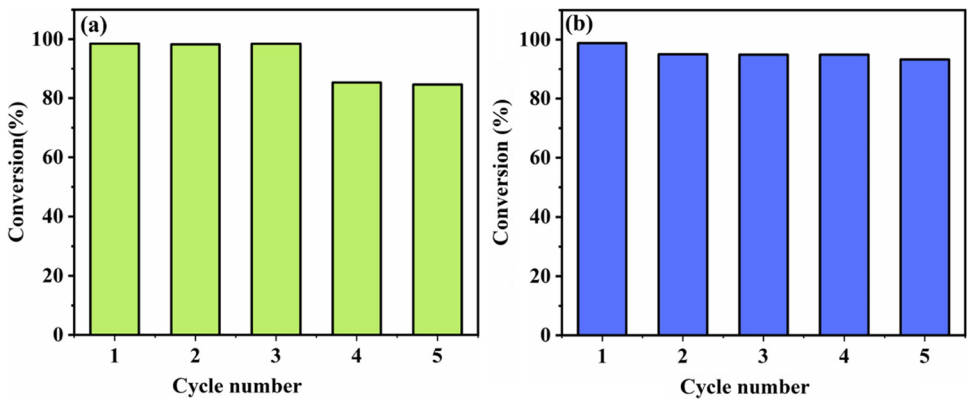

Fig. 9 The percent of conversion of **a** 4-NP and **b** MB solutions using recycled RGO/AgNPs nanohybrid for five consecutive cycles

Conclusions

In summary, amine-functionalized RGO-supported AgNPs having superior catalytic efficiency were synthesized by a simple and environmentally friendly approach. RGO/AgNPs nanohybrid was synthesized by a one-pot hydrothermal reduction of silver nitrate in the presence of APTMS-modified GO nanosheets and it was successfully characterized by using XRD, SEM, TEM, FT-IR, and Raman spectroscopy techniques. The $-NH_2$ groups on the surface of APTMS-modified GO act as effective and well-organized nucleation centers facilitating uniform growth of discrete and smaller-sized spherical AgNPs on the surface of RGO nanosheets. The catalytic efficiency of RGO/AgNPs nanohybrid was evaluated for the reduction of 4-NP MB using $NaBH_4$ reductant at room temperature. The synergistic effects of RGO, APTMS, and Ag components endow superior catalytic activity to RGO/AgNPs nanohybrid. Here, RGO nanosheets function as an efficient supporting material for the uniform dispersion of AgNPs without aggregation thereby retaining their catalytic activity. RGO will also accelerate the catalytic reduction process by facilitating efficient adsorption of 4-NP and MB on its surface by π-π and electrostatic interactions. The electron donation by the $-NH_2$ groups of APTMS will increase the surface electron density of anchored AgNPs which will further augment the catalytic activity of the developed RGO/AgNPs nanohybrid. Accordingly, RGO/AgNPs nanohybrid developed in the present study exhibited superior catalytic activity towards the reduction of 4-NP and MB in comparison with previously reported graphene/graphene oxide/reduced graphene oxide-supported AgNPs catalysts. The catalytic reduction of 4-NP

and MB followed pseudo-unimolecular kinetics in the present study and the rate constants were found to be 18.83 × 10^{-3} s^{-1} and 131.5 ×10^{-3} s^{-1} respectively for 4-NP and MB. Additionally, RGO/AgNPs nanohybrid showed good recyclability with negligible loss in its activity up to five recycle runs. The excellent catalytic activity, favorable kinetic parameters, and sustained catalytic efficiency after recycling make the RGO/AgNPs nanohybrid a promising catalyst for the reduction of organic pollutants in wastewater treatment.

Supplementary Information The online version contains supplementary material available at https://doi.org/10.1007/s11356-023-29115-2.

Acknowledgements The authors would like to thank the SAIF-CUSAT for XRD, SEM, TEM, and FT-IR analysis. We also thank Sophisticated Instrumentation Centre, Kannur University for Raman analysis and UV-Vis absorption studies.

Author contribution All authors contributed to the study conception and design. This work was designed by Dr. Shima. P. Damodaran. The research work was executed by Vijina Chathambally with the support of Majitha Kundathil Purayil. The first draft of the manuscript was written by Vijina Chathambally and all authors commented on previous versions of the manuscript. All authors read and approved the final manuscript.

Declarations

Ethics approval and consent to participate Not applicable

Consent for publication Not applicable

Competing interests The authors declare no competing interests.

References

Adel M, Ahmed MA, Elabiad MA, Mohamed AA (2022) Removal of heavy metals and dyes from wastewater using graphene oxide-based nanomaterials: A critical review. Environ Nanotechnology, Monit Manag 18:100719. https://doi.org/10.1016/J.ENMM.2022.100719

Alipour N, Namazi H (2019) Polydopamine-graphene / Ag – Pd nanocomposite as sustainable catalyst for reduction of nitrophenol compounds and dyes in environment. Mater Chem Phys 234:38–47. https://doi.org/10.1016/j.matchemphys.2019.05.085

Bae S, Gim S, Kim H, Hanna K (2016) Effect of NaBH4 on properties of nanoscale zero-valent iron and its catalytic activity for reduction of p-nitrophenol. Appl Catal B Environ 182:541–549. https://doi.org/10.1016/J.APCATB.2015.10.006

Chen WQ, Li QT, Li PH et al (2015) In situ random co-polycondensation for preparation of reduced graphene oxide/polyimide nanocomposites with amino-modified and chemically reduced graphene oxide. J Mater Sci 50:3860–3874. https://doi.org/10.1007/s10853-015-8890-7

Chen X, Chen B (2018) Facile fabrication of crumpled graphene oxide nanosheets and its Platinum nanohybrids for high efficient catalytic activity. Environ Pollut 243:1810–1817. https://doi.org/10.1016/j.envpol.2018.10.009

Damodaran SP (2021) Novel Nanohybrid Containing Magnetite Nanocluster-Decorated Reduced Graphene Oxide Nanosheets for Heat Transfer Applications. ChemistrySelect 6:6698–6706. https://doi.org/10.1002/slct.202101692

Das TK, Ghosh SK, Das NC (2023) Green synthesis of a reduced graphene oxide/silver nanoparticles-based catalyst for degradation of a wide range of organic pollutants. Nano-Struct Nano-Objects 34. https://doi.org/10.1016/j.nanoso.2023.100960

Dat NM, Long PNB, Nhi DCU et al (2020) Synthesis of silver/reduced graphene oxide for antibacterial activity and catalytic reduction of organic dyes. Synth Met 260:116260. https://doi.org/10.1016/J.SYNTHMET.2019.116260

Doan VD, Nguyen NV, Nguyen TLH et al (2021) High-efficient reduction of methylene blue and 4-nitrophenol by silver nanoparticles embedded in magnetic graphene oxide. Environ Sci Pollut Res. https://doi.org/10.1007/s11356-021-13597-z

Dong L, Yu W, Liu M et al (2019) Novel Composite Electrode of the Reduced Graphene Oxide Nanosheets with Gold Nanoparticles Modified by Glucose Oxidase for Electrochemical Reactions. Catalysts 9:764. https://doi.org/10.3390/catal9090764

Han X (2023) Ag-Ni alloy nanoparticles decorated reduced graphene oxide nanocomposite as highly efficient recyclable catalyst for the reduction of 4-nitrophenol and methylene blue. J Sol-Gel Sci Technol 105(3):836–847. https://doi.org/10.1007/s10971-023-06055-4

Han XW, Guo S, Li T et al (2022) Construction of Ag/3D-reduced graphene oxide nanocomposite with advanced catalytic capacity for 4-nitrophenol and methylene blue. Colloids Surf A Physicochem Eng Asp 650:128688. https://doi.org/10.1016/J.COLSURFA.2022.128688

Hareesh HK, Joshi RP, D.V. S, et al (2016) Anchoring of Ag-Au alloy nanoparticles on reduced graphene oxide sheets for the reduction of 4-nitrophenol. Appl Surf Sci 389:1050–1055. https://doi.org/10.1016/j.apsusc.2016.08.034

Hashemi Salehi M, Yousefi M, Hekmati M, Balali E (2019) Application of palladium nanoparticle-decorated Artemisia abrotanum extract-modified graphene oxide for highly active catalytic reduction of methylene blue, methyl orange and rhodamine B. Appl Organomet Chem 33:1–6. https://doi.org/10.1002/aoc.5123

He C, Liu Z, Lu Y et al (2016) Graphene-supported silver nanoparticles with high activities toward chemical catalytic reduction of methylene blue and electrocatalytic oxidation of hydrazine. Int J Electrochem Sci 11:9566–9574. https://doi.org/10.20964/2016.11.72

Hervés P, Pérez-Lorenzo M, Liz-Marzán LM et al (2012) Catalysis by metallic nanoparticles in aqueous solution: Model reactions. Chem Soc Rev 41:5577–5587. https://doi.org/10.1039/c2cs35029g

Hummers WS, Offeman RE (1958) Preparation of Graphitic Oxide. J Am Chem Soc 80:1339. https://doi.org/10.1021/ja01539a017

Iqbal M, Taiba A, Muhammad N et al (2021) Synthesis and Characterization of rGO / Ag 2 O Nanocomposite and its Use for Catalytic Reduction of 4 - Nitrophenol and Photocatalytic Activity. J Inorg Organomet Polym Mater 31:100–111. https://doi.org/10.1007/s10904-020-01680-w

Jiang ZJ, Liu CY, Sun LW (2005) Catalytic properties of silver nanoparticles supported on silica spheres. J Phys Chem B 109:1730–1735. https://doi.org/10.1021/jp046032g

K R, Palantavida S, Vijayan BK (2019) A Facile Method for the Synthesis of CuO-RGO Nanocomposite for Para Nitrophenol Reduction Reaction. Mater Today Proc 9:587–593. https://doi.org/10.1016/j.matpr.2018.10.379

Karczmarska A, Adamek M, El Houbbadi S et al (2022) Carbon-Supported Noble-Metal Nanoparticles for Catalytic Applications—A Review. Crystals 12:584. https://doi.org/10.3390/cryst12050584

Katheresan V, Kansedo J, Lau SY (2018) Efficiency of various recent wastewater dye removal methods: A review. J Environ Chem Eng 6:4676–4697. https://doi.org/10.1016/J.JECE.2018.06.060

Khan I, Saeed K, Zekker I et al (2022) Review on Methylene Blue: Its Properties, Uses, Toxicity and Photodegradation. Water 14:242. https://doi.org/10.3390/w14020242

Kolya H, Kuila T, Hoon N, Hee J (2019) Bioinspired silver nanoparticles / reduced graphene oxide nanocomposites for catalytic

reduction of 4-nitrophenol , organic dyes and act as energy storage electrode material. Compos Part B 173:106924. https://doi.org/10.1016/j.compositesb.2019.106924

Krishna R, Fernandes DM, Dias C et al (2016) Facile synthesis of Co/RGO nanocomposite for methylene blue dye removal. Mater Today Proc 3:2814–2821. https://doi.org/10.1016/j.matpr.2016.06.031

Li J, Liu CY, Liu Y (2012) Au/graphene hydrogel: Synthesis, characterization and its use for catalytic reduction of 4-nitrophenol. J Mater Chem 22:8426–8430. https://doi.org/10.1039/c2jm16386a

Li N, Zhang F, Wang H, Hou S (2019) Catalytic Degradation of 4-Nitrophenol in Polluted Water by Three-Dimensional Gold Nanoparticles / Reduced Graphene Oxide Microspheres. https://doi.org/10.30919/es8d509

Low SK, Tan MC (2018) Journal of Environmental Chemical Engineering Dye adsorption characteristic of ultrasound pre-treated pomelo peel. J Environ Chem Eng 6:3502–3509. https://doi.org/10.1016/j.jece.2018.05.013

Mohammadi Z, Entezari MH (2018) Sono-synthesis approach in uniform loading of ultrafine Ag nanoparticles on reduced graphene oxide nanosheets: An efficient catalyst for the reduction of 4-Nitrophenol. Ultrason Sonochem 44:1–13. https://doi.org/10.1016/j.ultsonch.2018.01.020

Ndolomingo MJ, Bingwa N, Meijboom R (2020) Review of supported metal nanoparticles: synthesis methodologies, advantages and application as catalysts. J Mater Sci 55:6195–6241. https://doi.org/10.1007/s10853-020-04415-x

Nezamzadeh-Ejhieh A, Khorsandi S (2014) Photocatalytic degradation of 4-nitrophenol with ZnO supported nano-clinoptilolite zeolite. J Ind Eng Chem 20:937–946. https://doi.org/10.1016/j.jiec.2013.06.026

Nimita Jebaranjitham J, Mageshwari C, Saravanan R, Mu N (2019) Fabrication of amine functionalized graphene oxide – AgNPs nanocomposite with improved dispersibility for reduction of 4-nitrophenol. Compos Part B Eng 171:302–309. https://doi.org/10.1016/j.compositesb.2019.05.018

Pandey PC, Shukla S, Pandey Y (2016) 3-Aminopropyltrimethoxysilane and graphene oxide/reduced graphene oxide-induced generation of gold nanoparticles and their nanocomposites: Electrocatalytic and kinetic activity. RSC Adv 6:80549–80556. https://doi.org/10.1039/c6ra18731e

Patel P, Maliekal PJ, Lingayat S, Badani PM (2022) Understanding the Kinetics and Reduction of Methylene Blue Using NaBH4. Russ J Phys Chem B 16:869–876. https://doi.org/10.1134/S1990793122050074

Revathy TA, Dhanavel S, Sivaranjani T et al (2018) Applied Surface Science Highly active graphene-supported palladium-nickel alloy nanoparticles for catalytic reduction of 4-nitrophenol. Appl Surf Sci 449:764–771. https://doi.org/10.1016/j.apsusc.2018.01.280

Saha J, Begum A, Mukherjee A, Kumar S (2017) A novel green synthesis of silver nanoparticles and their catalytic action in reduction of Methylene Blue dye. Sustain Environ Res 27:245–250. https://doi.org/10.1016/j.serj.2017.04.003

Sahu D, Sahoo G, Mohapatra P, Swain SK (2019) Dual Activities of Nano Silver Embedded Reduced Graphene Oxide Using Clove Leaf Extracts: Hg 2+ Sensing and Catalytic Degradation. ChemistrySelect 4:2593–2602. https://doi.org/10.1002/slct.201803725

Saptal VB, Saptal MV, Mane RS et al (2019) Amine-Functionalized Graphene Oxide-Stabilized Pd Nanoparticles (Pd@APGO): A Novel and Efficient Catalyst for the Suzuki and Carbonylative Suzuki-Miyaura Coupling Reactions. ACS Omega 4:643–649. https://doi.org/10.1021/acsomega.8b03023

Shaker Ardakani L, Surendar A, Thangavelu L, Mandal T (2021) Silver nanoparticles (Ag NPs) as catalyst in chemical reactions. Synth Commun 51:1–21. https://doi.org/10.1080/00397911.2021.1894450

Sponza DT, Kuscu ÖS (2011) Relationships between acute toxicities of para nitrophenol (p-NP) and nitrobenzene (NB) to Daphnia magna and Photobacterium phosphoreum: Physicochemical properties and metabolites under anaerobic/aerobic sequentials. J Hazard Mater 185:1187–1197. https://doi.org/10.1016/j.jhazmat.2010.10.030

Sreekanth TVM, Jung MJ, Eom IY (2016) Green synthesis of silver nanoparticles, decorated on graphene oxide nanosheets and their catalytic activity. Appl Surf Sci 361:102–106. https://doi.org/10.1016/j.apsusc.2015.11.146

Svalova A, Brusko V, Sultanova E et al (2021) Individual Ni atoms on reduced graphene oxide as efficient catalytic system for reduction of 4-nitrophenol. Appl Surf Sci 565:150503. https://doi.org/10.1016/j.apsusc.2021.150503

Thu TV, Ko PJ, Van Nguyen T et al (2017) Green synthesis of reduced graphene oxide/Fe3O4/Ag ternary nanohybrid and its application as magnetically recoverable catalyst in the reduction of 4-nitrophenol. Appl Organomet Chem 31:1–9. https://doi.org/10.1002/aoc.3781

Tran XT, Hussain M, Kim HT (2020) Facile and fast synthesis of a reduced graphene oxide/carbon nanotube/iron/silver hybrid and its enhanced performance in catalytic reduction of 4–nitrophenol. Solid State Sci 100:106107. https://doi.org/10.1016/j.solidstatesciences.2019.106107

Trikkaliotis DG, Christoforidis AK, Mitropoulos AC, Kyzas GZ (2021) Graphene Oxide Synthesis , Properties and Characterization Techniques : A Comprehensive Review. ChemEngineering 5(3):64

Trikkaliotis DG, Mitropoulos AC, Kyzas GZ (2020) Low-cost route for top-down synthesis of over- and low-oxidized graphene oxide. Colloids Surfaces A 600:124928. https://doi.org/10.1016/j.colsurfa.2020.124928

Vinothkannan M, Karthikeyan C, Gnana Kumar G et al (2015) One-pot green synthesis of reduced graphene oxide (RGO)/Fe3O4 nanocomposites and its catalytic activity toward methylene blue dye degradation. Spectrochim Acta - Part A Mol Biomol Spectrosc 136:256–264. https://doi.org/10.1016/j.saa.2014.09.031

Wang Z, Xu C, Gao G, Li X (2014) Facile synthesis of well-dispersed Pd-graphene nanohybrids and their catalytic properties in 4-nitrophenol reduction. RSC Adv 4:13644–13651. https://doi.org/10.1039/c3ra47721e

Wang Z, Xu C, Li X, Liu Z (2015) In situ green synthesis of Ag nanoparticles on tea polyphenols-modified graphene and their catalytic reduction activity of 4-nitrophenol. Colloids Surf A Physicochem Eng Asp 485:102–110. https://doi.org/10.1016/j.colsurfa.2015.09.015

Xie Y, Liu B, Li Y et al (2019) Cu/Cu2O/rGO nanocomposites: Solid-state self-reduction synthesis and catalytic activity for: P -nitrophenol reduction. New J Chem 43:12118–12125. https://doi.org/10.1039/c9nj02768h

Yu W (2020) RSC Advances Progress in the functional modi fi cation of graphene / graphene oxide : a review, pp 15328–15345. https://doi.org/10.1039/d0ra01068e

Zarei M, Seyedi N, Maghsoudi S et al (2021) Green synthesis of Ag nanoparticles on the modified graphene oxide using Capparis spinosa fruit extract for catalytic reduction of organic dyes. Inorg Chem Commun 123:108327. https://doi.org/10.1016/j.inoche.2020.108327

Zelechowska K, Kondratowicz I, Gazda M (2016) Graphene hydrogels with embedded metal nanoparticles as efficient catalysts in 4-nitrophenol reduction and methylene blue decolorization. Polish J Chem Technol 18:47–55. https://doi.org/10.1515/pjct-2016-0070

Zhang AX, Zhu X, Feng J, Wang A (2017) Solvothermal synthesis of N-doped graphene supported PtCo nanodendrites with highly catalytic activity for 4-nitrophenol reduction. Appl Surf Sci. https://doi.org/10.1016/j.apsusc.2017.09.200

Zhou S, Ji H, Fu Y et al (2020) Mussel-inspired fabrication of cationic polymer modified rGO supported silver nanoparticles hybrid with robust antibacterial and catalytic reduction performance. Appl Surf Sci 506:144655. https://doi.org/10.1016/J.APSUSC.2019.144655